ACS SENSORS

Article

Cite This: ACS Sens. 2018, 3, 618–623

pubs.acs.org/acssensors

Si Nanostrip Optical Waveguide for On-Chip Broadband Molecular Overtone Spectroscopy in Near-Infrared

Aviad Katiyi and Alina Karabchevsky*

Electrooptical Engineering Unit , Ben-Gurion University of the Negev, David Ben Gurion Blvd, P.O. Box 653, Beer-Sheva 8410501, Israel

Ilse Katz Institute for Nanoscale Science & Technology, Ben-Gurion University of the Negev, David Ben Gurion Blvd, P.O. Box 653, Beer-Sheva 8410501, Israel

Center for Quantum Information Science and Technology, Ben-Gurion University of the Negev, David Ben Gurion Blvd, P.O. Box 653, Beer-Sheva 8410501, Israel

ABSTRACT: The ability to probe the molecular fundamental or overtone (high harmonics) vibrations is fundamental to modern healthcare monitoring techniques and sensing technologies since it provides information about the molecular structure. However, since the absorption cross section of molecular vibration overtones is much smaller compared to the absorption cross section of fundamental vibrations, their detection is challenging. Here, a silicon nanostrip rib waveguide structure is proposed for label-free on-chip overtone spectroscopy in near-infrared (NIR). Utilizing the large refractive index contrast ($\Delta n > 2$) between the silicon core of the waveguide and the silica substrate, a broadband NIR lightwave can be efficiently guided. We show that the sensitivity for chemical detection is increased by more than 3 orders of magnitude when compared to the evanescent-wave sensing predicted by the numerical model. This spectrometer distinguished several common organic liquids such as *N*-methylaniline and aniline precisely without any surface modification to the waveguide through the waveguide scanning over the absorption dips in the NIR transmission spectra. Planar NIR Si nanostrip waveguide is a compact sensor that can provide a platform for accurate chemical detection. Our NIR Si nanostrip rib waveguide device can enable the development of sensors for remote, on-site monitoring of chemicals.

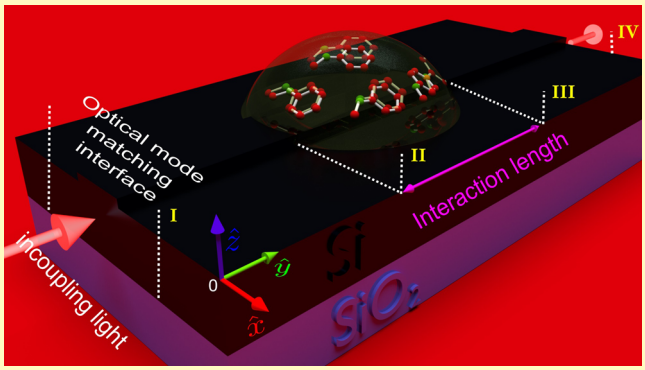

KEYWORDS: *molecular vibrations, overtones, near-infrared, waveguide, on-chip, nanosensor*

Spectroscopy focuses on the interaction between light and matter. This interaction results in absorption or emission of radiation due to the change in molecular energy. The energy appears in different regions of the electromagnetic spectrum and gives distinctive information about the molecular structure therefore, infrared spectroscopy is certainly one of the most important analytical techniques available to today's scientists. In the mid-infrared (MIR) region of the electromagnetic spectrum, the fundamental vibrations can be excited, resulting in well pronounced absorption lines that mitigate the identification of molecular bonds. However, their high molecular absorption coefficient prevents large penetration depth and an adjustment of sample thickness. As opposed to the MIR, near-infrared (NIR) radiation excites overtone and combination vibrational modes and allows direct analysis of strongly absorbing and highly scattering samples without further pretreatments. Albeit, absorption cross section of molecular vibration overtones is much smaller compared to the fundamental vibrations and therefore molecular vibration overtones are challenging to detect.

Optical waveguides platform[1] operating in NIR region can be used for remote and on-site detection in applications such as monitoring urban pollutants, toxins, volatile industrial elements, and certain military threats. The major drawback of current sensors is the specificity requirement determined by the functionalization of the sensor's surface. This additional process of surface modification is aimed at identification of specific chemicals. For instance, refractometers are sensors, which rely on a change in refractive index,[2−6] and therefore they lack in identification of unlabeled analytes and bioentities since the refractive index of many of them could be similar. In addition, many different biochemical species coexist in a biological sample and these species register nearly indistinguishable shifts of refractive index when adsorbed onto the sensors. This results in a difficulty of multichannel detection of group of analytes since different areas of such sensor have to be differently prepared or pretreated with different antibodies[7−9] or markers.

Received: November 22, 2017
Accepted: February 13, 2018
Published: February 13, 2018

DOI: 10.1021/acssensors.7b00867
ACS Sens. 2018, 3, 618–623

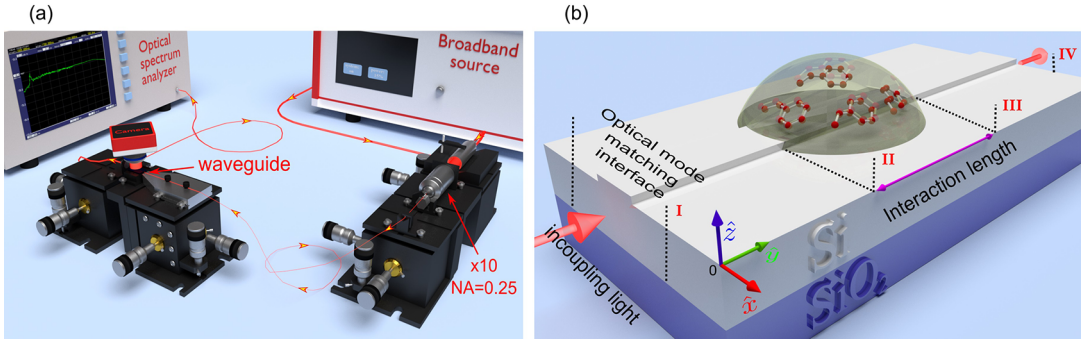

Figure 1. (a) Illustration of the experimental setup. Broadband NIR laser source is coupled to the single-mode fiber using a microscope objective. The fiber is butt-coupled to the input facet of the waveguide. The output signal is collected by the multimode fiber into the optical spectrum analyzer. The waveguides are imaged on the camera for the inspection, characterization and alignment. The propagation direction of light is indicated by the arrows. (b) Schematic of a Si nanostrip rib structure. Incident light illuminates the waveguide facet. The liquid is placed on the waveguide within the interaction length where the optical absorption for spectrum scanning takes place.

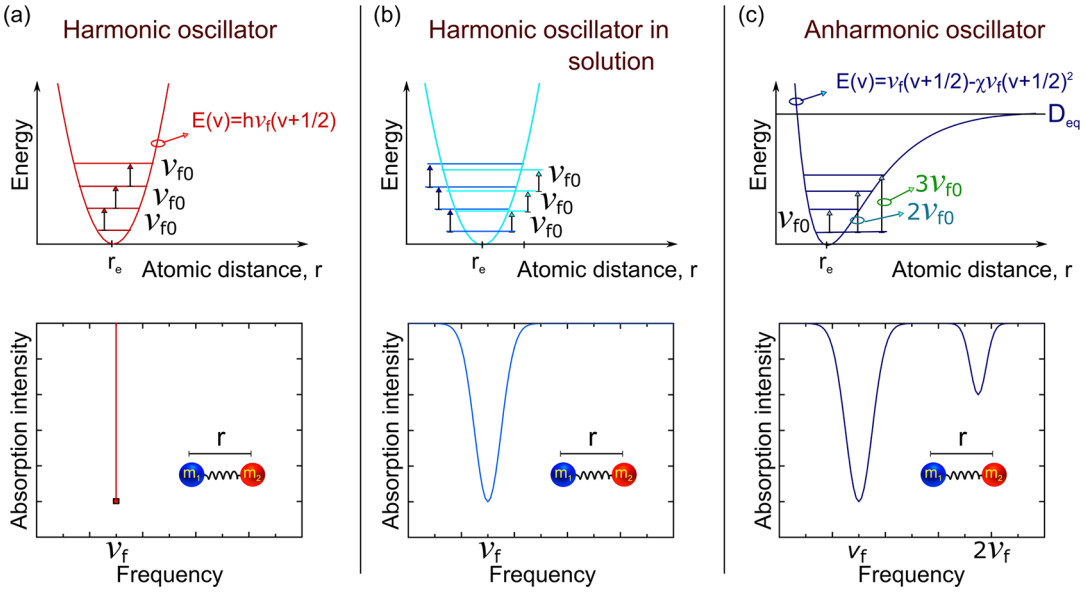

Figure 2. Diagrams of an oscillator mechanism described by the energy levels (top) and the corresponding spectral transmittance patterns (bottom) for (a) harmonic oscillator, (b) harmonic oscillator with the heterogeneity of the medium, and (c) anharmonic oscillator. Dissociation energy and the equilibrium bond distance are indicated by D_e and r_e, respectively.

Microresonator based sensing architectures,[10−13] in contrast, demonstrate high sensitivity at a specific wavelength. However, due to the inherent property of the narrow free spectral range (FSR), these devices cannot provide broadband sensing.[14] Mid-infrared spectroscopy is an efficient detection method which allows for label-free sensing.[15−17] In contrast to the sensing techniques mentioned above, mid-infrared radiation is absorbed by molecular bonds, resulting in well-defined fundamental vibrations represented by absorption bands in the spectrum.[18] Common equipment such as Fourier transform infrared (FTIR) spectrometers[19,20] or wavelength scanning monochromators show mid-infrared spectra but they are bulky and much larger than a chip-scale sensor. Chip-scale mid-infrared sensors were reported[21,22] for detection of common chemicals such as *N*-bromohexane, toluene, and isopropanol. Near-infrared spectrophotometers are widely used for acquiring near-infrared spectra using a cuvette as a liquid reservoir. Similar to the FTIR spectrometer, near-infrared spectrophotometers use benchtop equipment that is too large for monolithic integration on a chip. Chalcogenide waveguides[23] were proposed to probe molecular overtones in near-infrared while integrated with microfluidic chip. Glass-based waveguides showed well-defined amine overtone absorption band around 1.5 μm in the diffusive regime.[24] However, these waveguides were pretreated by negative charge using plasma oxygen which is not suitable for on-site long-time measurements.

Here, we present a new chip-scale photonic device that utilizes NIR absorption by molecular vibration overtones for label-free chemical sensing. We designed a multimode silicon nanostrip waveguide in such a way, that launching the high order modes improves the sensitivity of the chip-scale device for broadband detection. Reducing the height of the nanostrip will prevent the excitation of high order modes and affect the sensitivity. We experimentally demonstrate that this NIR on-chip sensor can distinguish between different organic liquids. Our NIR Si nanostrip rib waveguide device can enable the development of sensors for remote, on-site monitoring of chemicals and more.

DOI: 10.1021/acssensors.7b00867
ACS Sens. 2018, 3, 618−623

RESULTS AND DISCUSSION

Figure 1a shows an illustration of our experimental setup for the demonstration of the effect. The broadband laser source (Fianium WL-SC-400-15) was coupled to a single-mode fiber. The fiber was held with a piezoelectric stage which allows for precise adjustment of the fiber to the waveguide. The output signal was collected via multimode fiber into an optical spectrum analyzer (Yokogawa AQ6370D). The waveguide surface was imaged onto a camera of the inverted microscope for the accurate inspection.

The proposed sensor shown in Figure 1b has dimensions of 5 mm (L) × 5 mm (W) × 1 mm (D) and supports nine guided modes. Due to the large evanescent field and increased interaction with the analyte, high order modes contribute to the sensitivity of the sensor. We found that, in Si nanostrip configuration, the sensitivity of the sensor does not change beyond nine modes. The effect of enhanced NIR absorption was realized in butt-coupled experiments. To demonstrate the effect, the sensor was butt-coupled to the single-mode fiber and illuminated by the broadband source. The broadband source allows for identifying multiple absorption bands and enables identification of multiple bonds in the analyte. Although sophisticated on-chip spectrometers have been demonstrated in MIR[21] and NIR,[1,14,23,24] broadband NIR spectrometers have never been shown for detection of molecular vibration overtones for spectral tracing with Si nanostrip.

It is known that the NIR spectroscopy is based on molecular overtones and combination modes vibrations with transitions which are forbidden by the selection rules of quantum mechanics.[25] Transition probability $R_{i,j}$ describes the possibility of transition from lower i to higher j energy level defined by

$$R_{i,j} \propto \int \psi_i M \psi_j d \tag{1}$$

with wave function ψ and transition moment operator M. Due to the selection rule, only transition of $\Delta\nu = \pm 1$ is allowed in the harmonic oscillator model. The energy differences between the adjacent energy levels are constant, resulting in the absorption of only a photon with the exact energy that fits the frequency of the oscillator, ν_0, as shown in Figure 2a. The frequency that leads to the transition from $\nu = 0$ to $\nu = 1$ is the fundamental frequency.

Ideally, in the harmonic model, the absorption spectra occur at a discrete frequency with zero width (Figure 2a). However, in practice, the absorption has nonzero width along the spectrum (Figure 2b). This occurs because the harmonic model describes a single diatomic molecule or identical diatomic molecules. In practice, the diatomic molecules are not identical because they are embedded in a heterogeneous solution. For this reason, a molecule is influenced slightly differently by the surroundings. As a result, the vibration frequency for the same transition, for example the fundamental frequency, is a little shifted in different molecules, resulting in broadening of the absorption as shown in Figure 2b. Anharmonic models influence the spectra in few ways. First, the energy differences between the adjacent energy levels are slightly different. This results in a group of absorptions of the same $\Delta\nu$ (for example: 0 → 1, 1 → 2, and 2 → 3), which results in broadening of the spectral line. Second, the transition rule of the harmonic model is not applied in the anharmonic model, which allows vibration transitions of $\Delta\nu \neq 1$. Few absorption bands will appear in the spectrum, as shown in Figure 2c. The frequencies that result in those transitions are called overtones or higher harmonics and they are the topic of this paper. Due to the lower probability of the overtone transitions, the first overtone is smaller by a factor of 10 compared to the fundamental transition.[26] The probability of higher order overtones transitions also decreases as factor 10, therefore, detection of molecular overtones is challenging.[26] As mentioned above, the great advantage of the NIR spectroscopy is the large penetration depth into the analyte. Therefore, broadband NIR spectroscopy can be very useful in probing bulk material without special sample preparation, surface functionalization or surface treatment.

In this paper, we describe NIR transparent chip-based device that utilizes an optical nanostrip rib waveguide to guide a broadband light for efficient monitoring of analytes. We suggest a new approach that can allow the NIR light to interact with bulk analyte and efficiently excite molecular vibration overtones. This device provides improvements over current evanescent-wave detection using diffused waveguides,[24] ring resonators,[14] or channel waveguides[1,23] in three ways: (1) the availability in detection over a broad spectral range (from λ = 1.1 μm to λ = 1.65 μm), (2) efficient coupling to high order modes significantly enhances the interaction between the evanescent field and the analyte and imparts high sensitivity to this device, and (3) no need of surface treatment.

In Figure 1a, we illustrate the structure of the NIR silicon nanostrip sensor device. The sensing element is a nanostrip rib waveguide with two end-facets butt-coupled to optical fibers. The optical fiber is launched into the nanostrip rib waveguide. The hydrophibicity of the device due to the 2 nm thick layer of the native oxide on Si, confines the liquids within the interaction length. Thus, the Si nanostrip rib structure serves as (a) an efficient NIR medium for transmitting the NIR light and (b) fluid confining element. After passing through the interaction length, the NIR probe light contains the fingerprint of the analyte as an absorption bands. It is subsequently recorded by a vis/near-IR optical spectrum analyzer. The transmitted light contains the absorption spectrum of the analyte. Each absorption band is related to different atomic bonds in the analyte.

To illustrate the layout of the NIR nanostrip rib waveguides and their corresponding NIR response, we highlight four interfaces (Figure 1a): (I) the infacet where the in-coupling light from the optical fiber couples to the waveguide, (II) and (III) the interfaces between the waveguide and the analyte, and (IV) the endfacet where the out-coupling light from the waveguide couples to the optical fiber. The waveguide guiding layer is made of silicon and the substrate is made of silica. The sensing area is located within the interaction length and between interface II and III. The guidance is provided by total internal reflection at the interfaces with air and the SiO_2 substrate. The total broadband optical transmittance of the device is defined primarily by the losses of the power within the interaction length and therefore is obtained as in ref 27:

$$T = \left| \sum_{\gamma 1 = 0,1,..,8} C_{\gamma 1} \exp(-1\alpha_{\gamma 1} L) \right|^2 \tag{2}$$

where $C_{\gamma 1} = (I_{\gamma 0,\gamma 1} + I_{\gamma 1,\gamma 0})^2/(4I_{\gamma 0,\gamma 0} I_{\gamma 1},\gamma 1)$ and L is the interaction length. α is an attenuation coefficient in dB/cm of modes[27] in a region filled with the analyte $0 < y < L$, and $\gamma 0$ = 0,1,.., 8 are the guided modes in regions I,II and $\gamma 1$ = 0,1,.., 8 are the guided modes in regions II,III influenced by the analyte.

DOI: 10.1021/acssensors.7b00867
ACS Sens. 2018, 3, 618−623

Figure 3 shows scanning electron microscopy (SEM) images of the fabricated Si nanostrip rib waveguides. A clearly resolved

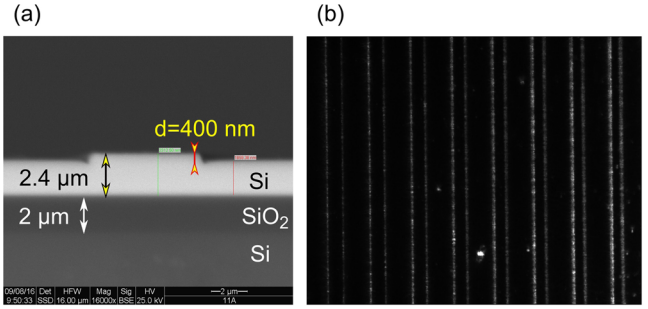

Figure 3. Images of the Si nanostrip waveguide. (a) SEM image of the waveguide cross section. (b) Top view of the rib waveguide showing the scattering effect of waveguide walls.

400 nm thick nanostrip is etched on the Si forming the Si layer of 2.4 μm. Then 2 μm silica layer is sandwiched between the guiding layer and the silicon substrate to fulfill the guidance condition. Figure 3b shows a top view of the rib waveguides of different widths of the strip. The scattered light is due to the roughness of the waveguide walls.

The chemical sensitivity of our rib nanostrip waveguide[28] was simulated using finite-difference time-domain (FDTD) and finite-element method (FEM) numerical solvers. We determined sensitivity by calculating the fraction of the evanescent field:

$$\eta_{\text{evanes}} = \frac{P_{\text{analyte}}}{P_{\text{total}}} = \frac{\int\int_{\text{analyte}} \mathcal{S}\, dA}{\int\int_{-\infty}^{\infty} \mathcal{S}\, dA} \tag{3}$$

With time varying Poynting vector $\mathcal{S}$ defined as

$$\mathcal{S} = \frac{1}{2}\Re\{EH^*\} \tag{4}$$

The absorption is caused due to the excitation of molecular vibration overtone, mathematically described by the complex refractive index of the liquid; therefore, the electric E and magnetic H fields in a waveguide evolve as complex.

Using FDTD solver, we studied the modes and their absorption for rib waveguide at wavelength of 1.5 μm. Higher order modes have greater absorption here, due to the strong evanescent field. Figure 4a and b shows the predicted optical field profiles (TE and TM, respectively) for propagating NIR radiation, wavelength of λ = 1.5 μm within a rib waveguide with pure N-methylaniline as analyte. Figure 4c and d shows the absorption of TE modes and TM modes, respectively.

Figure 4a and b shows that in the silicon rib waveguide the fundamental mode is highly confined at the center of the waveguide core and interacts weakly with the analyte for both TE and TM modes. In addition, it is shown in Figure 4c and d that the absorbance for a low order modes in the silicon rib waveguide have very low absorption. Thus, exciting higher order modes will contribute to the enhancement of the evanescent field, which consequently improves the sensitivity of the sensor.[1]

It is important to understand the evolution of the modes due to the abrupt discontinuity in the medium in which the nanostrip is embedded. Specifically, the abrupt change in the medium affects the guided modes, resulting in a unique spectral

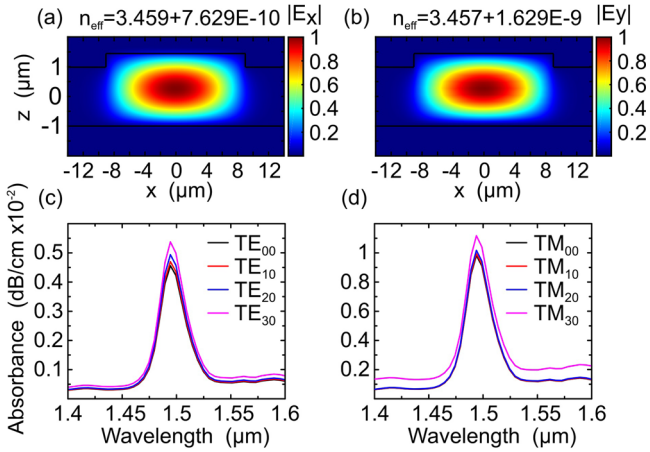

Figure 4. Calculated normalized fundamental mode intensity profile of a Si nanostrip rib waveguide at λ = 1.5 μm of (a) fundamental TE and (b) fundamental TM. (c) Absorbance of $TE_{\gamma 1,n}$ modes. (d) Absorbance of $TM_{\gamma 1,n}$ modes. Note: For here $\gamma 1$ = 0, 1, 2, 3 for simplicity of visualization. However, the calculations were performed for all nine $\gamma 1$ = 0,1.., 8 modes.

signature of the molecule under investigation. Figure 5 shows the cross section color maps of the evolution of normalized

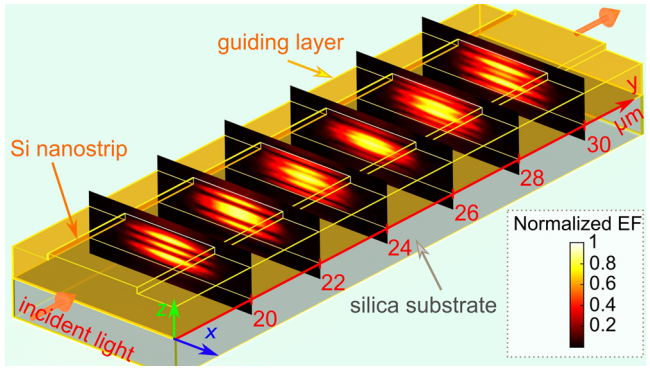

Figure 5. Evolution of the interfered guided modes in the interaction length with the analyte. Calculated normalized mode profiles using FDTD, with different distance d from the beginning of the interaction region at the point of y = II. d is indicated on each subplot. The amplitude of normalized electric field (EF) is presented in the inset.

mode profiles exhibiting interference and guided in the interaction length of the designed waveguide (Figure 1a). A Gaussian beam, wavelength of 1.5 μm, radius of 4.75 μm, and divergence angle of 0.13 rad, was launched into the waveguide. The analyte was explored at a distance d of y = 10 μm from the waveguide infacet at the point of y = I. In the simulation $y(I)$ = 0, the cross sections of the calculated normalized mode profiles were performed at distances of y = 20, 22,.., 30 μm with an interval of 2 μm from the beginning of the interaction length at the point of y = II as shown in Figure 5.

For the validation of the proposed structure as efficient near-infrared sensor, we explored N-methylaniline, aniline, and mixture of N-methylaniline in hexane. These analytes have absorption bands of the first overtone of the amine group N−H around 1.5 μm.[29] During the experiment, the analyte with volume of 3 μL was dripped into the waveguide surface defining the interaction length of 2 mm. Figure 6 shows the

DOI: 10.1021/acssensors.7b00867
ACS Sens. 2018, 3, 618−623

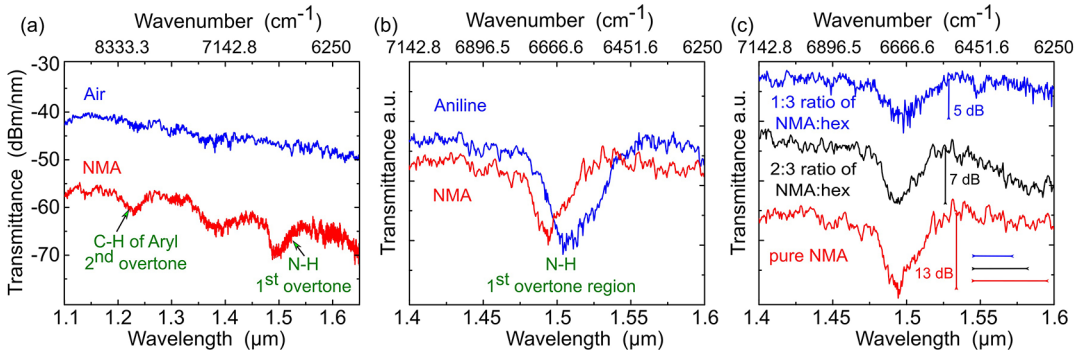

Figure 6. Spectral characterizations using on-chip Si nanostrip rib waveguide NIR spectrometer. (a) Transmittance spectra of pure *N*-methylaniline (NMA). As a reference, we measured the transmittance through the waveguide in air. (b) Transmittance spectra of *N*-methylaniline and aniline. (c) Transmittance spectra of pure *N*-methylaniline molecule and mixture ratios of 1:3 and 2:3 of *N*-methylaniline in hexane, NMA/hex, with indicated absorption depths of the analytes. In addition, the bars are placed next to each other for clear comparison of absorption depths.

experimental results performed on silicon nanostrip rib waveguide experiments.

Figure 6a shows absorption bands of *N*-methylaniline around 1.5 and 1.2 μm which correspond to the molecule vibrational modes of first N−H overtone and second C−H overtone,[30] respectively. Figure 6b clearly shows differences in the transmission of *N*-methylaniline and aniline. The absorption bands of first overtone of N−H in *N*-methylaniline and aniline was successfully detected around 1.5 μm. The absorption band of aniline is wider compared to the absorption band of *N*-methylaniline. The broadening of aniline absorption on the N−H first overtone can be explained by the excitation of combination molecular vibrational modes.[29,31] Figure 6c shows the transmission spectra of the pure *N*-methylaniline molecule and mixture ratios 1:3 and 2:3 of NMA/hexane. It demonstrates the ability to detect and study the absorption of different mixtures ratio of NMA/hexane using a silicon rib waveguide. The waveguide is illuminated by the optical fiber with angular divergence, and therefore with other modes (orthogonal to each other) coexisting. Each optical mode has a discrete propagation constant β. The coupling efficiencies (from fiber to waveguides) including the insertion and propagation losses were −30 dB. Even with obtaining such a high loss, the molecular signature overtones were detected on the devices reported here.

CONCLUSIONS

In conclusion, we proposed a silicon nanostrip rib waveguide structure for label-free on-chip overtone spectroscopy in NIR. We show that, utilizing the large refractive index contrast ($\Delta n > 2$) between the Si core of the waveguide and the SiO_2 substrate, a broadband NIR lightwave can be efficiently guided. In addition, we show that the sensitivity for chemical detection is increased by more than 3 orders of magnitude when compared to the evanescent-wave sensing predicted by the numerical model. Our on-chip spectrometer distinguished several common organic liquids such as *N*-methylaniline and aniline precisely without any guide's surface modification through the spectral scanning over the absorption dips in the NIR transmission spectra. Planar NIR silicon nanostrip waveguide is a compact sensor which can provide a platform for accurate chemical detection. Our NIR silicon nanostrip rib waveguide device can enable the development of sensors for remote, on-site monitoring of chemicals.

MATERIALS AND METHODS

Chemicals. Aniline ($C_6H_5NH_2$, ≥99.5%), hexane (C_6H_{14}, ≥95%), and *N*-methylaniline ($C_6H_5NH(CH_3)$, ≥98%) were purchased from Sigma-Aldrich.

Fabrication. Silicon layer was e-beam evaporated on silicon wafer. The rib patterns were first created with conventional photolithography and then etched.

Waveguide Characterization. We measured the waveguide dimension using a Stylus Profilometer, Veeco Dektak-8.

Simulation. The three-dimensional simulation was performed using a commercial Maxwell solver: Lumerical FDTD (Finite Difference Time Domain) solutions.

Spectroscopy on a Waveguide. The broadband laser source (Fianium WL-SC-400-15), bandwidth from 450 to 2400 nm, was focused into the single mode fiber (1550BHP) using an X10 plan achromat objective (Olympus) with a numerical aperture of NA = 0.25. The fiber was aligned with the waveguide using a stereo microscope (Zeiss Stemi SV6). The spectra were collected using the multimode fiber into the optical spectrum analyzer (Yokogawa 6370D).

AUTHOR INFORMATION

Corresponding Author

*E-mail: alinak@bgu.ac.il.

ORCID

Aviad Katiyi: 0000-0002-7924-9065

Alina Karabchevsky: 0000-0002-4338-349X

Notes

The authors declare no competing financial interest.

ACKNOWLEDGMENTS

The authors acknowledge the support of the Multidisciplinary Program Health-Engineering Sciences grant by the Ben-Gurion University of the Negev. The authors thank Dr. Avi Niv for kindly lending the supercontinuum light source to perform the measurements. The authors also acknowledge the help of Benyimin Hadad in obtaining the SEM images.

REFERENCES

(1) Katiyi, A.; Karabchevsky, A. Figure of merit of all-dielectric waveguide structures for absorption overtone spectroscopy. *J. Lightwave Technol.* **2017**, *35*, 2902−2908.

(2) Karabchevsky, A.; Tsapovsky, L.; Marks, R. S.; Abdulhalim, I. Study of immobilization procedure on silver nanolayers and detection of estrone with diverged beam surface plasmon resonance (SPR) imaging. *Biosensors* **2013**, *3*, 157−170.

DOI: 10.1021/acssensors.7b00867
ACS Sens. 2018, 3, 618−623

(3) Karabchevsky, A.; Karabchevsky, S.; Abdulhalim, I. Nano-precision algorithm for surface plasmon resonance determination from images with low contrast for improved sensor resolution. *J. Nanophotonics* **2011**, *5*, 051813.
(4) Karabchevsky, A.; Karabchevsky, S.; Abdulhalim, I. Fast surface plasmon resonance imaging sensor using Radon transform. *Sens. Actuators, B* **2011**, *155*, 361−365.
(5) Wang, Q.; Farrell, G. All-fiber multimode-interference-based refractometer sensor: proposal and design. *Opt. Lett.* **2006**, *31*, 317−319.
(6) Schroeder, K.; Ecke, W.; Mueller, R.; Willsch, R.; Andreev, A. A fibre Bragg grating refractometer. *Meas. Sci. Technol.* **2001**, *12*, 757.
(7) Shia, W. W.; Bailey, R. C. Single domain antibodies for the detection of ricin using silicon photonic microring resonator arrays. *Anal. Chem.* **2013**, *85*, 805−810.
(8) Kurihara, Y.; Takama, M.; Sekiya, T.; Yoshihara, Y.; Ooya, T.; Takeuchi, T. Fabrication of carboxylated silicon nitride sensor chips for detection of antigen-antibody reaction using microfluidic reflectometric interference spectroscopy. *Langmuir* **2012**, *28*, 13609−13615.
(9) Tromberg, B. J.; Sepaniak, M. J.; Alarie, J. P.; Tuan, V. D.; Santella, R. M. Development of antibody-based fiber-optic sensors for detection of a benzo [a] pyrene metabolite. *Anal. Chem.* **1988**, *60*, 1901−1908.
(10) Wan, J.; Johnson, M. L.; Guntupalli, R.; Petrenko, V. A.; Chin, B. A. Detection of Bacillus anthracis spores in liquid using phage-based magnetoelastic micro-resonators. *Sens. Actuators, B* **2007**, *127*, 559−566.
(11) Ksendzov, A.; Lin, Y. Integrated optics ring-resonator sensors for protein detection. *Opt. Lett.* **2005**, *30*, 3344−3346.
(12) Sumetsky, M.; Windeler, R.; Dulashko, Y.; Fan, X. Optical liquid ring resonator sensor. *Opt. Express* **2007**, *15*, 14376−14381.
(13) Li, M.; Wu, X.; Liu, L.; Fan, X.; Xu, L. Self-referencing optofluidic ring resonator sensor for highly sensitive biomolecular detection. *Anal. Chem.* **2013**, *85*, 9328−9332.
(14) Nitkowski, A.; Chen, L.; Lipson, M. Cavity-enhanced on-chip absorption spectroscopy using microring resonators. *Opt. Express* **2008**, *16*, 11930−11936.
(15) Jin, T.; Li, L.; Zhang, B.; Lin, H.-Y. G.; Wang, H.; Lin, P. T. Real-Time and Label-Free Chemical Sensor-on-a-chip using Monolithic Si-on-BaTiO 3 Mid-Infrared waveguides. *Sci. Rep.* **2017**, *7*, 1−8.
(16) Lin, P. T.; Giammarco, J.; Borodinov, N.; Savchak, M.; Singh, V.; Kimerling, L. C.; Tan, D. T.; Richardson, K. A.; Luzinov, I.; Agarwal, A. Label-Free Water Sensors Using Hybrid Polymer-Dielectric Mid-Infrared Optical Waveguides. *ACS Appl. Mater. Interfaces* **2015**, *7*, 11189−11194.
(17) Wang, X.; Antoszewski, J.; Putrino, G.; Lei, W.; Faraone, L.; Mizaikoff, B. Mercury-cadmium-telluride waveguides-a novel strategy for on-chip mid-infrared sensors. *Anal. Chem.* **2013**, *85*, 10648−10652.
(18) Vajda, V.; Pucetaite, M.; McLoughlin, S.; Engdahl, A.; Heimdal, J.; Uvdal, P. Molecular signatures of fossil leaves provide unexpected new evidence for extinct plant relationships. *Nature ecology & evolution* **2017**, *1*, 1093−1099.
(19) Bhargava, R.; Levin, I. W. Fourier transform infrared imaging: theory and practice. *Anal. Chem.* **2001**, *73*, 5157−5167.
(20) Griffiths, P. R.; De Haseth, J. A. *Fourier transform infrared spectrometry*; John Wiley & Sons, 2007; Vol. *171*.
(21) Lin, P. T.; Kwok, S. W.; Lin, H.-Y. G.; Singh, V.; Kimerling, L. C.; Whitesides, G. M.; Agarwal, A. Mid-infrared spectrometer using opto-nanofluidic slot-waveguide for label-free on-chip chemical sensing. *Nano Lett.* **2014**, *14*, 231−238.
(22) Yu, C.; Ganjoo, A.; Jain, H.; Pantano, C.; Irudayaraj, J. Mid-IR biosensor: detection and fingerprinting of pathogens on gold island functionalized chalcogenide films. *Anal. Chem.* **2006**, *78*, 2500−2506.
(23) Hu, J.; Tarasov, V.; Agarwal, A.; Kimerling, L.; Carlie, N.; Petit, L.; Richardson, K. Fabrication and testing of planar chalcogenide waveguide integrated microfluidic sensor. *Opt. Express* **2007**, *15*, 2307−2314.
(24) Karabchevsky, A.; Kavokin, A. Giant absorption of light by molecular vibrations on a chip. *Sci. Rep.* **2016**, *6*, 1−7.
(25) Atkins, P. W.; Friedman, R. S. *Molecular quantum mechanics*; Oxford University Press, 2011.
(26) Suart, B. *Infrared Spectroscopy: Fundamental and Applications*; John Wiley & Sons, Ltd, 2004.
(27) Karabchevsky, A.; Wilkinson, J. S.; Zervas, M. N. Transmittance and surface intensity in 3D composite plasmonic waveguides. *Opt. Express* **2015**, *23*, 14407−14423.
(28) Okamoto, K. *Fundamentals of optical waveguides*; Academic Press, 2010.
(29) Whetsel, K. B.; Roberson, W. E.; Krell, M. Near-infrared spectra of primary aromatic amines. *Anal. Chem.* **1958**, *30*, 1598−1604.
(30) Shaji, S.; Eappen, S. M.; Rasheed, T.; Nair, K. NIR vibrational overtone spectra of N-methylaniline, N, N-dimethylaniline and N, N-diethylaniline-a conformational structural analysis using local mode model. *Spectrochim. Acta, Part A* **2004**, *60*, 351−355.
(31) Shaji, S.; Rasheed, T. Vibrational overtone spectra of chloroanilines-evidence for intramolecular hydrogen bonding in o-chloroaniline. *Spectrochim. Acta, Part A* **2001**, *57*, 337−347.

DOI: 10.1021/acssensors.7b00867
ACS Sens. 2018, 3, 618−623